DESIGN BUCKLING CURVES FOR CLAMPED ORTHOTROPIC LAMINATED PLATES

Nicholas G. Tsouvalis[1] and Vassilios J. Papazoglou[2]

[1] Assistant Professor, [2] Professor
School of Naval Architecture and Marine Engineering, National Technical University of Athens
9 Heroon Polytechniou Str., Zografos, GR 157-73, Greece

ABSTRACT

Non-dimensional design buckling curves for clamped rectangular orthotropic plates are presented in this study. These curves provide the critical buckling load of thin, symmetric, cross-ply laminated plates as a function of the laminate's rigidities and aspect ratio for the following seven configurations of the applied in-plane loads: uniform uniaxial compression, triangular uniaxial compression, uniaxial in-plane bending, pure shear, uniform uniaxial compression combined with shear, triangular uniaxial compression combined with shear, and uniaxial in-plane bending combined with shear. Approximate mathematical formulae are also provided. The Classical Lamination Theory, in conjunction with the Rayleigh-Ritz method, has been used for the determination of the critical buckling load. The validity of the study is confirmed by comparing its results with other both theoretical and numerical ones.

1. INTRODUCTION

The avoidance of buckling failure possesses a predominant place among the structural design criteria any structure should fulfil. This requirement becomes of vital importance in FRP structures, due to the much higher flexibility of composite materials as compared to the traditional metallic ones, owing to their lower moduli of elasticity. Regarding the specific field of FRP marine structures, local buckling of laminated plates between the various longitudinal and transverse stiffeners is the first failure mode that should be expected in a poorly designed vessel, since almost all structural plates in a ship hull are subjected one way or another to various in-plane loads. These may be uniformly distributed compressive or tensile loads, like those at the bottom or deck plating due to hogging and sagging; shear loads combined with in-plane bending, like those at the hull sides; or, uniform compressive loads combined with shear, like those at the transverse bulkheads.

Considerable effort has been spent in the past trying to identify the structural response of either isotropic or anisotropic laminated plates under the action of various types of in-plane loads. The majority of these works concerns bifurcation-type buckling of plates subjected to uniform compression and/or shear loading, with considerable less attention being given to clamped plates with other types and combinations of loads. Such classical and typical works include [1], [2], [3] and [4].

To help the designer in applying a rational structural design approach, non-dimensional bending and buckling curves have been derived in the past for either isotropic or laminated plates ([5], [6]). However, these curves do not cover a satisfactory range of load cases and, additionally, they are not very accurate, especially those for pure shear loading and those in cases of significant orthotropy and large aspect ratios. It is the purpose of this study to present non-dimensional design buckling curves for clamped, symmetric, specially orthotropic or cross-ply laminated composite plates. These curves provide the critical buckling load of the laminate as a function of its rigidities and aspect ratio for the following seven configurations of the applied in-plane loads: (a) uniform uniaxial compression, (b) triangular uniaxial compression, (c) uniaxial in-plane bending, (d) pure shear, (e) uniform uniaxial compression combined with shear, (f) triangular uniaxial compression combined with shear and (g) uniaxial in-plane bending combined with shear.

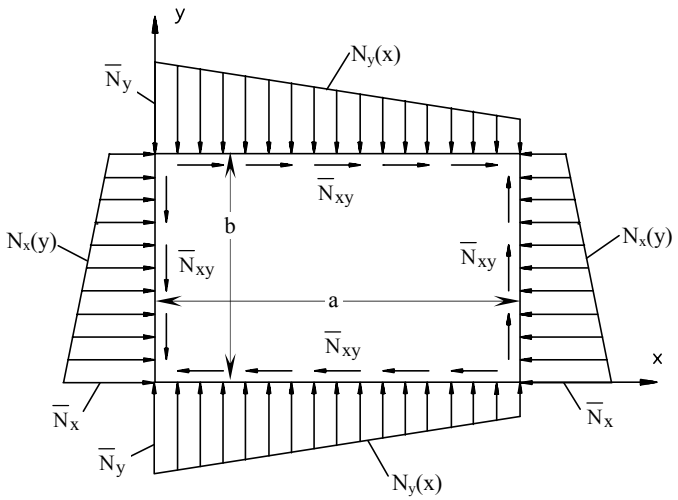

Fig. 1. Laminate geometry and loading configuration.

Fig. 2. Loading form for various values of coefficient φ_1.

2. THEORETICAL MODELING

The Classical Lamination Theory (CLT), in conjunction with the Rayleigh-Ritz method, was used for the calculation of the critical buckling load values. The laminate geometry and loading condition taken into account is shown in Fig. 1. All loads shown in this figure are considered positive. Shear load $\overline{N}_{xy}$ remains constant, whereas axial loads $N_x(y)$ and $N_y(x)$ vary along the edges of the laminate according to the following linear equations:

$$N_x(y) = \overline{N}_x\left(1-\varphi_1\frac{y}{b}\right) \quad , \quad N_y(x) = \overline{N}_y\left(1-\varphi_2\frac{x}{a}\right) \tag{1}$$

The value of coefficients φ_1 and φ_2 in Eq. (1) define the form of the linearly varying loads. Thus, $\varphi_1 = 0$ results in a uniform load, $0 < \varphi_1 < 1$ results in a trapezoidal load, $\varphi_1 = 1$ results in a triangular load and $\varphi_1 = 2$ results in in-plane bending of the laminate (see Fig. 2). Analogous load forms are also valid for $N_y(x)$, by varying coefficient φ_2.

The determination of the critical buckling load was performed with the aid of the well known Rayleigh-Ritz energy method. According to CLT, the potential energy Π of the laminate can be expressed as [7]:

$$\Pi = \frac{1}{2}\int_0^a\int_0^b\left[\boldsymbol{N}_x\frac{\partial u}{\partial x}+\boldsymbol{N}_y\frac{\partial v}{\partial y}+\boldsymbol{N}_{xy}\left(\frac{\partial u}{\partial y}+\frac{\partial v}{\partial x}\right)-\boldsymbol{M}_x\frac{\partial^2 w}{\partial x^2}-\boldsymbol{M}_y\frac{\partial^2 w}{\partial y^2}-2\boldsymbol{M}_{xy}\frac{\partial^2 w}{\partial x\,\partial y}\right]dx\,dy$$
$$-\frac{1}{2}\int_0^a\int_0^b\left[N_x\left(\frac{\partial w}{\partial x}\right)^2+2\overline{N}_{xy}\frac{\partial w}{\partial x}\frac{\partial w}{\partial y}+N_y\left(\frac{\partial w}{\partial y}\right)^2\right]dx\,dy \tag{2}$$

where a and b are the dimensions of the laminate (see Fig. 1), $\boldsymbol{N}_i$ and $\boldsymbol{M}_i$ are the stress and moment resultants in the laminate geometrical axes, u, v and w are the midplane

displacements in the x, y and z directions respectively, and N_x, N_y and $\overline{N}_{xy}$ are the externally applied loads per unit length shown in Fig. 1.
The boundary conditions of a fully clamped laminate is expressed by the well know equations w = 0 and $\partial w/\partial n = 0$, where n is the direction normal to the laminate edge. According to the Rayleigh-Ritz method, appropriate deflection functions are selected for the three displacements u, v and w, capable of satisfying the boundary conditions and leading to acceptably accurate results. For unsymmetric cross-ply laminates, the following three equations fulfil the above requirements and therefore are selected for application [8]:

$$u_o(x,y) = \sum_{m=1}^{\infty}\sum_{n=1}^{\infty} U_{mn} \sin\frac{m\pi x}{a} \cos\frac{n\pi y}{b} \tag{3}$$

$$v_o(x,y) = \sum_{m=1}^{\infty}\sum_{n=1}^{\infty} V_{mn} \cos\frac{m\pi x}{a} \sin\frac{n\pi y}{b} \tag{4}$$

$$w_o(x,y) = \sum_{m=1}^{\infty}\sum_{n=1}^{\infty} W_{mn} \; X_m(x) \; Y_n(y) \tag{5}$$

where m and n are half-wavelength integers, U_{mn}, V_{mn} and W_{mn} the undetermined coefficients, and functions $X_m(x)$ and $Y_n(y)$ are given by:

$$X_m(x) = \cosh\left(a_m \frac{x}{a}\right) - \cos\left(a_m \frac{x}{a}\right) - \gamma_m \left[\sinh\left(a_m \frac{x}{a}\right) - \sin\left(a_m \frac{x}{a}\right)\right] \tag{6}$$

$$Y_n(y) = \cosh\left(a_n \frac{y}{b}\right) - \cos\left(a_n \frac{y}{b}\right) - \gamma_n \left[\sinh\left(a_n \frac{y}{b}\right) - \sin\left(a_n \frac{y}{b}\right)\right] \tag{7}$$

The values of arithmetic coefficients a_i and γ_i are given in [8].
According to the least potential energy theorem, from all displacement fields that satisfy the compatibility equations and the specific boundary conditions, those satisfying also the equilibrium equations minimize the potential energy. This is mathematically expressed by setting the variation of the potential energy equal to zero, that is $\delta\Pi = 0$. After extensive algebra, this expression results in an equation of the following form:

$$\delta\Pi = \sum_{m=1}^{m_f}\sum_{n=1}^{n_f}\left[(...)\,\delta U_{mn} + (...)\,\delta V_{mn} + (...)\,\delta W_{mn}\right] = 0 \tag{8}$$

Setting the coefficients of δU_{mn}, δV_{mn} and δW_{mn} equal to zero, leads to three sets of simultaneous algebraic equations. Considering that integer indices m and n in Eq. (3) to (5) belong into close intervals [1, m_f] and [1, n_f] respectively, a set of $(3 \cdot m_f \cdot n_f)$ homogeneous equations in U_{mn}, V_{mn} and W_{mn} is produced, which, in contracted form, can be written as:

$$[A]\{x\} - \overline{N}_x [B]\{x\} = 0 \tag{9}$$

In the above equation [A] and [B] are real symmetric matrices and {x} is a column matrix containing the coefficients U_{mn}, V_{mn} and W_{mn}, that is giving the modeshape of the buckled laminate. Magnitude $\overline{N}_x$ is the unknown critical value of the applied load in the x direction (see Fig. 1). Note that loads $\overline{N}_y$ and $\overline{N}_{xy}$ have been taken into account through load ratios a_1 and a_2 defined as:

$$a_1 = \overline{N}_y / \overline{N}_x \qquad \text{and} \qquad a_2 = \overline{N}_{xy} / \overline{N}_x \tag{10}$$

Elements of matrix [A] in Eq. (9) are functions of the laminate stiffnesses and dimensions, whereas elements of matrix [B] are functions of the laminate dimensions, load coefficients φ_1 and φ_2, and load ratios a_1 and a_2. Eq. (9) is an expression of a generalized eigenvalue problem, which was solved using standard subroutines available in the literature [9].

3. VERIFICATION OF THE METHOD

The validity of the above theoretical model for buckling of clamped plates has been confirmed by comparing the obtained results to others available in the literature, as well as to the results of a respective finite element study. The first comparison was made for thin isotropic plates with various aspect ratios that are under the action of uniform uniaxial compression or pure shear, giving negligible differences between the present method and the results in reference [5]. A comparison with a semi numerical modeling [10] was also made for an isotropic plate with various aspect ratios in uniform uniaxial compression, resulting again in very small differences, less than 3%. Negligible differences were also found by comparing the results of the present method to those of reference [4] for square symmetric specially orthotropic laminates under uniform uniaxial compression. Regarding other types of loading, a comparison was made with the results of reference [11] for a square isotropic plate under the action of biaxial uniform compression with $\overline{N}_x = \overline{N}_y$. Once more the difference was less than 1%. Finally, very small differences were also obtained in the case of a square isotropic plate under the action of pure in-plane bending (φ_1=2) [12].

The effort of verifying the validity of the developed method was completed by comparing results of the theoretical model to respective ones obtained from the application of the finite element method. The widely used general purpose finite element code ALGOR was used for the determination of the eigenvalue load of an isotropic and a homogeneous orthotropic plate with aspect ratio equal to 2. The dimensions of the plates are 2 m by 1 m, the thickness being equal to 0.01 m. The material properties are E=207 GPa and ν=0.3 for the isotropic plate and E_1=120 GPa, E_2=30 GPa, G_{12}=5 GPa and ν_{12}=0.28 for the orthotropic plate. The model comprised of 5000 4-node, common rectangular plate elements, in association with either the isotropic or the orthotropic linear material model. The loading was imposed by means of a series of concentrated loads acting on the edges of the plate, their magnitudes determined using a consistent formulation. Four load cases were investigated, namely uniform uniaxial compression, triangular uniaxial compression, in-plane bending and pure shear (see Fig. 1). The results of this comparison are presented in Table 1, from which the excellent correlation becomes evident. All analytical results in Table 1 have been calculated taking $m_f = n_f = 9$ in Eq. (8), that is 81 terms for each displacement series expansion. A sample modeshape is given in Fig. 3 for the load case of the isotropic plate under in-plane bending.

4. DESIGN CURVES

The development of design curves which express the mechanical behaviour of structural

Table 1. Critical buckling load $\overline{N}_x$, in kN/m.

Loading	Isotropic Plate			Orthotropic Plate		
	Analytical	F.E.	Diff. (%)	Analytical	F.E.	Diff. (%)
Uniform uniaxial	1472.1	1475.0	0.2	346.7	347.2	0.1
Triangular uniaxial	2836.2	2841.7	0.2	665.3	666.1	0.1
In-plane bending	7792.8	7828.1	0.5	1747.7	1822.1	4.2
Pure shear	1920.3	1958.6	2.0	327.1	341.2	4.3

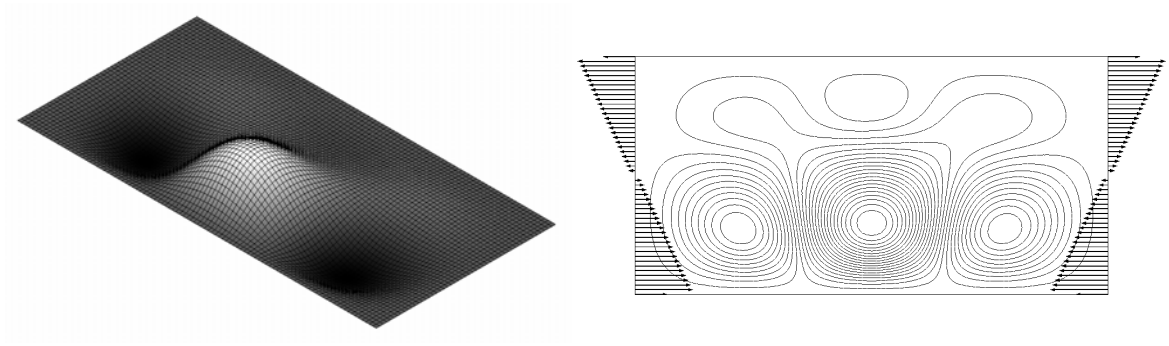

Fig. 3. Buckling modeshape of an orthotropic plate under in-plane bending.

members like plates or beams, includes most of the times the need for establishing various non-dimensional parameters, which are capable of adequately describing the whole problem. The design curves are then plotted as a function of these parameters and thus their validity is generic. In the case of plate buckling, the main parameters defining the phenomenon are the plate dimensions, the material properties and the critical buckling load. In the particular case of laminated plates, a magnitude is needed for incorporating and successfully expressing the layer material properties, the stacking sequence and the thickness and orientation of each ply. Such a magnitude can be only a function of the laminate bending stiffnesses D_{ij}.
The non-dimensional parameters used in this study have been taken into account in the work of other investigators too ([6], [13], [14]), who presented results for either stiffened isotropic or laminated plates. They have been also used by the authors in an earlier work to express the buckling behaviour of simply supported laminated plates [15]. The non-dimensional parameters are three and are given by the following expressions:

$$\eta = \frac{D_{12} + 2D_{66}}{\sqrt{D_{11} D_{22}}} \quad , \quad \rho = \frac{a}{b}\sqrt[4]{\frac{D_{22}}{D_{11}}} \quad , \quad \overline{N}_{x,cr} = k\frac{\pi^2\sqrt{D_{11} D_{22}}}{b^2} \tag{11}$$

Eq. (11) introduces the so called *generalized rigidity ratio* η, expressing the material properties lay out, the laminate *affine aspect ratio* ρ, describing the laminate geometry, and the critical value of the in-plane load in the x direction $\overline{N}_{x,cr}$. Coefficient k in the last of Eq. (11) is the non-dimensional buckling coefficient, given by the developed design curves.
Emphasis should be given to the range of variation of parameters η and ρ. According to [6], the generalized rigidity ratio varies between zero and one, with isotropic materials having η=1.0. High orthotropy, expressed by high values of ratio E_1/E_2, corresponds to low values of parameter η. In the present study, parameter η has been taken to vary between 0.2 and 1.0, thus covering almost all known specially orthotropic materials. However, buckling calculations can be performed for any value of parameter η, in the load cases where approximate formulae are given in the following. Regarding affine aspect ratio ρ, it has been taken to vary between 0.25 and 4.0. Taking into account that ratio D_{22}/D_{11} in Eq. (11) is smaller than unity, ρ = 4.0 actually corresponds to higher geometric aspect ratios.
All design buckling curves cited in the following have been calculated considering 81 terms in each displacement series expansion. Fig. 4 gives results for laminates under uniform uniaxial compression, presenting the variation of the critical buckling coefficient k of Eq. (11) versus the affine aspect ratio ρ, for various values of the generalized rigidity ratio η. Analyzing the data of Fig. 4 it was found that the critical buckling coefficient for values of parameter η different than unity can be expressed as a function of the corresponding critical buckling coefficient for η = 1.0, $k_{(\eta=1)}$, by the following equation:

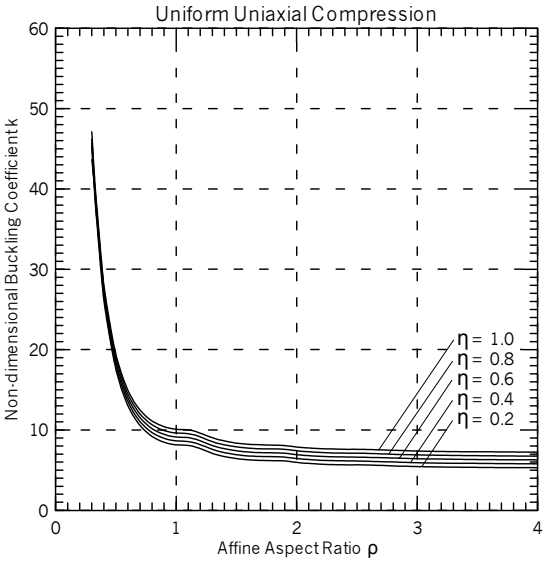

Fig. 4. Critical buckling coefficient k for clamped laminates under uniform uniaxial compression.

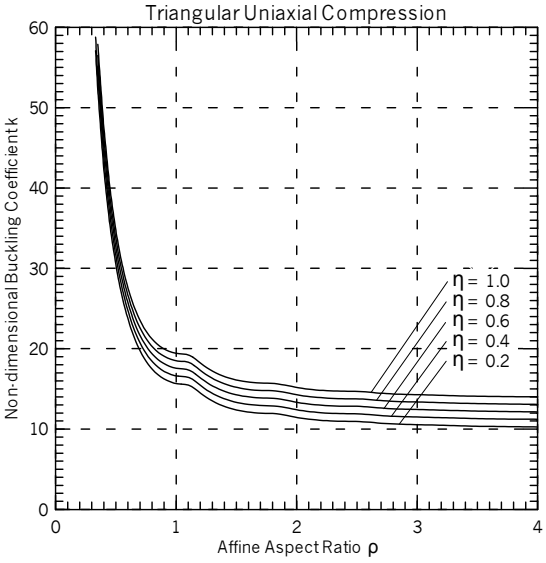

Fig. 5. Critical buckling coefficient k for clamped laminates under triangular uniaxial compression.

$$k = (-0.06\,\eta + 1.02)\,k_{(\eta=1)} + (3.04\,\eta - 2.64) \tag{12}$$

The accuracy of Eq. (12) is excellent, since its error is less than 2.2%.
In the case of laminates under triangular uniaxial compression (φ_1=1), corresponding results for the critical buckling coefficient are given in Fig. 5. Once more, an approximate mathematical expression was derived giving the magnitude of coefficient k for values of parameter η other than unity, as a function of coefficient k for η=1.0. The error of this approximation is very small, as in the previous load case. This expression is as follows:

$$k = (0.07\,\eta + 0.93)\,k_{(\eta=1)} + (3.44\,\eta - 3.47) \tag{13}$$

The critical buckling coefficient k for the load case of uniaxial in-plane bending (φ_1=2) is given in Fig. 6 for various values of parameter η. The formula expressing coefficient k for values of parameter η other than unity, as a function of coefficient k for η=1.0, is as follows:

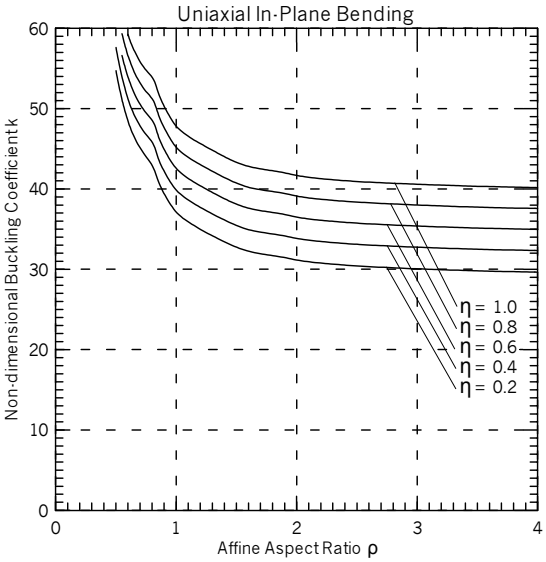

Fig. 6. Critical buckling coefficient k for clamped laminates under uniaxial in-plane bending.

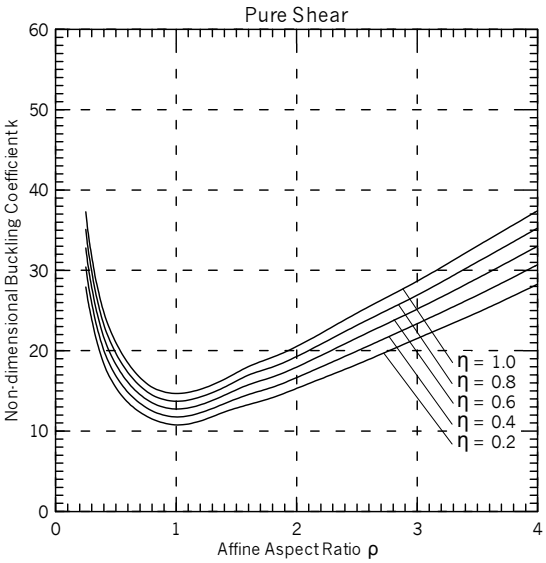

Fig. 7. Critical buckling coefficient k for clamped laminates under pure shear.

$$k = (0.07\eta + 0.93)\, k_{(\eta=1)} + (9.85\eta - 9.81) \tag{14}$$

Finally, the load case of pure shear is covered by the critical buckling coefficients given in Fig. 7, as a function of parameter η. However, in this load case the critical buckling coefficient k is no longer defined as in Eq. (11), but as follows:

$$\overline{N}_{xy,cr} = k\, \frac{\pi^2 \sqrt{D_{11}\, D_{22}}}{a\, b} \tag{15}$$

where $\overline{N}_{xy,cr}$ is the critical value of the applied shear load per unit length (see Fig. 2). This happens because, in the case of pure shear, the previous definition of k by Eq. (11) does not lead to non-dimensional curves with generic validity for all combinations of parameters ρ, η and aspect ratio a/b. As in the other load cases, the formula expressing coefficient k for values of parameter η other than unity, as a function of coefficient k for η=1.0, is as follows:

$$k = (0.3\eta - 0.7)\, k_{(\eta=1)} + (0.41\eta^2 - 0.39) \tag{16}$$

The expression has become in this case quadratic with respect to parameter η.
A thorough study of the graphs given in figures 4 to 7 reveals that, for a constant affine aspect ratio ρ, buckling strength increases with increasing value of the generalized rigidity ratio η, whereas for constant η and ρ > 2, the critical buckling load does not change significantly as a function of the affine aspect ratio ρ.
In the load cases where combinations of uniaxial and shear loads are taken into account, the buckling behaviour of the laminate is presented in terms of non-dimensional interaction buckling curves. Sample such curves are presented in Fig. 8 for the load case of combined uniform uniaxial compression and shear. Fig. 8 contains five distinct interaction curves, each one corresponding to a different value of the affine aspect ratio ρ. These curves provide the variation of ratio $\overline{N}_x / \overline{N}_{xo}$ as a function of ratio $\overline{N}_{xy} / \overline{N}_{xyo}$, where $\overline{N}_x$ is the applied uniaxial compression, $\overline{N}_{xy}$ is the applied pure shear, $\overline{N}_{xo}$ is the critical uniaxial buckling load in the x direction when it acts alone and $\overline{N}_{xyo}$ is the critical buckling shear load when it also acts alone onto the laminate. Fig. 8 is valid for laminates with generalized rigidity ratio η equal to 0.6. Analogous figures exist for all other values of η considered in this study, namely 0.2, 0.4, 0.8 and 1.0. Due to lack of space here, these figures, together with all other relevant information, are included in the publicly available web site **www.naval.ntua.gr/buckling-curves**, which was specially constructed to include all the results of the present study. The site contains a brief summary of the study, nomenclature and definition of the various magnitudes, as well as the respective non-dimensional buckling curves for all seven load cases considered. In addition and for the combined load cases, it also contains arithmetic tables giving the offsets of the buckling interaction curves for much more values of the affine aspect ratio ρ than those presented in Fig. 8.
The interaction curves like those presented in Fig. 8 can be used in two ways. Firstly, knowing the value of any of the two loads $\overline{N}_x$ or $\overline{N}_{xy}$ applied to the laminate, one can determine the magnitude of the other load, which is the critical one for the stability of the laminate. Besides, knowing the magnitude of both loads $\overline{N}_x$ and $\overline{N}_{xy}$ applied to the laminate,

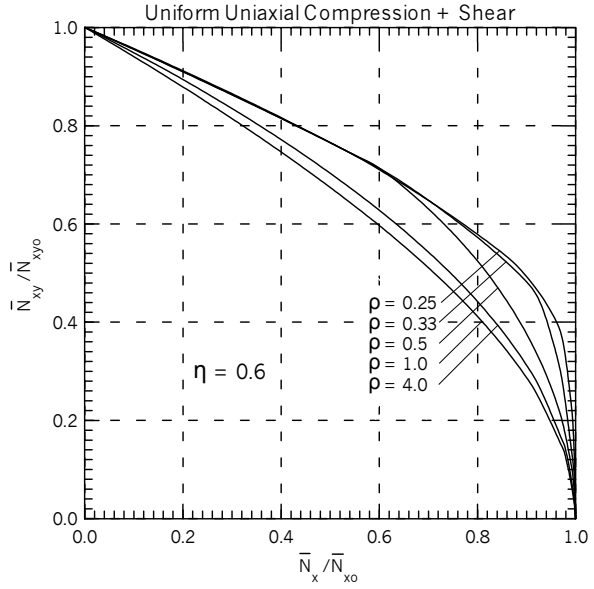

Fig. 8. Interaction buckling curves of clamped laminates under the combined action of uniform uniaxial compression and shear (η=0.6).

one can identify whether the laminate buckles or not under the action of these two particular loads. The area of the graph below each curve is the safe region, while any point above the curves corresponds to a pair of loads, whose combined application to the laminate causes its buckling failure. Sample interaction buckling curves for the load cases of triangular uniaxial compression and shear, and in-plane bending and shear are shown in figures 9 and 10, respectively, for η=0.6. It can be observed that the interaction curves are much smoother in these two latter load cases in comparison to those for the uniform uniaxial compression and shear, a behaviour indicating a smoother transition between the various mode shapes.

In order to facilitate the design procedure by providing the design engineers with easy to use tools for predicting the buckling behaviour of clamped composite laminated plates, an effort was made to describe this buckling behaviour by simple mathematical formulae. The study of

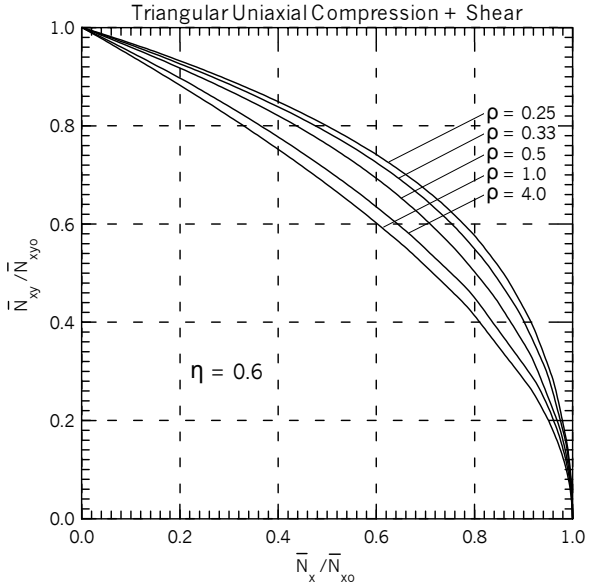

Fig. 9. Interaction buckling curves of clamped laminates under the combined action of triangular uniaxial compression and shear (η=0.6).

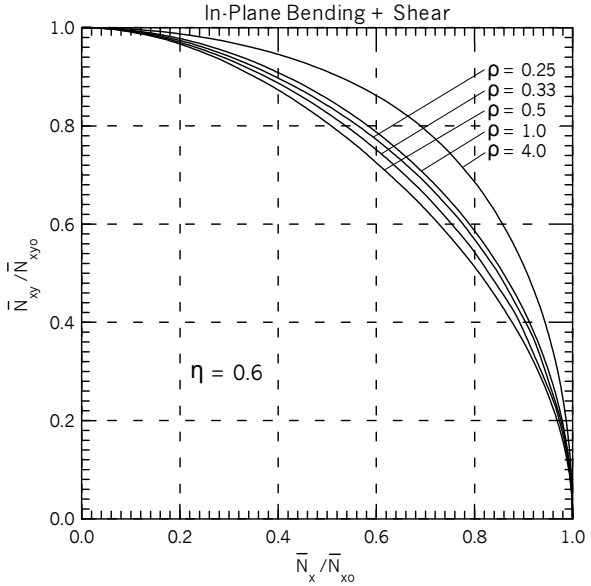

Fig. 10. Interaction buckling curves of clamped laminates under the combined action of uniaxial pure in-plane bending and shear (η=0.6).

Table 2. Superscripts p and q for the interaction buckling bounding curves of Eq.(17).

Loading	Minimum bounding curve		Maximum bounding curve	
	p	q	p	q
Uniform uniaxial and shear	0.94	1.87	0.75	3.50
Triangular uniaxial and shear	0.96	1.87	1.17	2.60
In-plane bending and shear	1.65	1.78	2.40	2.20

all interaction curves for all values of parameter η and all load cases contained in the aforementioned web site leads to the result that the curves are always within an envelope, limited by two curves that correspond to affine aspect ratios ρ which exhibit the minimum and maximum buckling strength, respectively. Thus, for uniform uniaxial compression and shear and for triangular uniaxial compression and shear the two bounding curves correspond to ρ=1.0 (the minimum) and ρ=0.25 (the maximum), whereas for in-plane bending and shear they correspond to ρ=0.5 (the minimum) and ρ=4.0 (the maximum). A statistical analysis of the offsets of these curves revealed that these bounding curves are approximately independent of the generalized rigidity ratio η; this is especially true for the lower bounding curve that corresponds to the minimum buckling strength. This statistical analysis resulted in the conclusion that these bounding curves can be represented by the general equation

$$\left(\frac{\overline{N}_x}{\overline{\overline{N}}_{xo}}\right)^p + \left(\frac{\overline{N}_{xy}}{\overline{\overline{N}}_{xyo}}\right)^q = 1 \qquad (17)$$

where superscripts p and q are defined in Table 2 for all load cases. These curves provide a very good approximation of the buckling behaviour of clamped composite laminated plates under the action of combined loading; especially the minimum bounding curve can be used for a safe prediction of this behaviour.

5. CONCLUSIONS

The present study provides the designer with all necessary means for performing any buckling calculation of a thin, symmetric, specially orthotropic composite laminated plate with clamped edges. This is done quite simply through the use of non-dimensional buckling curves giving the critical buckling load. The only input data needed are the laminate dimensions and bending rigidities. Many loading conditions have been taken into account, covering almost all common cases that could appear in marine and other structures. The provided approximate mathematical formulae simplify even further the calculation procedure, enabling it to constitute a very handy design tool.

References

1. **Bleich, F.**, "Buckling strength of metal structures", McGraw Hill Book Co., New York, 1961.
2. **Lekhnitskii, S.G.**, "Anisotropic plates", Gordon and Breach Science Publ., New York, 1968.
3. **Whitney, J.M.**, "The effect of boundary conditions on the response of laminated composites", *J Compos Mater*, **4** (1970), 192-203.
4. **Lagace, P.A.**, **Jensen, D.W.** and **Finch, D.C.**, "Buckling of unsymmetric composite laminates", *Compos Struct*, **5**/2 (1986), 101-123.
5. **Hughes, O.F.**, "Ship structural design: A rationally-based, computer aided, optimization approach", John Willey & Sons, New York, 1983.
6. **Brunelle, E.J.** and **Oyibo, G.A.**, "Generic buckling curves for specially orthotropic rectangular plates", *AIAA J*, **21**/8 (1983), 1150-1156.
7. **Papazoglou, V.J.**, **Tsouvalis, N.G.** and **Kyriakopoulos, G.D.**, "Buckling of unsymmetric laminates under linearly varying biaxial in-plane loads combined with shear", *Compos Struct*, **20**/2 (1992), 155-163.

8. **Chia, C.Y.** and **Prabhakara, M.K.**, "Postbuckling behaviour of unsymmetrically layered anisotropic rectangular plates", *J Appl Mech*, **41**/1 (1974), 155-162.
9. **Press, W.H.**, **Flannery, B.P.**, **et al** "Numerical Recipes: The Art of Scientific Computing", Cambridge Univ. Press, London, 1986.
10. **Harik, I.E.** and **Ekambaram, R.**, "Seminumerical solution for buckling of rectangular plates", *Comput Struct*, **23**/5 (1986), 649-655.
11. **Grimm, T.R.** and **Gerdeen, J.C.**, "Instability analysis of thin rectangular plates using the Kantorovich method", *J Appl Mech*, **42**/1 (1975), 110-114.
12. **Mukhopadhyay, M**, "Buckling analysis of rectangular ship plating", *Int'l Shipbuilding Progress*, May (1979), 89-97.
13. **Mansour, E.A.**, "Ship bottom structure under uniform lateral and in-plane loads", *Schiff und Hafen*, **5** (1967), 323-339.
14. **Brunelle, E.J.**, "The fundamental constants of orthotropic affine slab/plate equations", *AIAA J*, **23**/12 (1985), 1957-1961.
15. **Papazoglou, V.J.** and **Tsouvalis, N.G.**, "Design curves for specially orthotropic laminated plates under combined in-plane loading", *Transactions of the Society of Naval Architects and Marine Engineers (SNAME)*, **99** (1991), 377-403.